

## Photodissociation of C–H and C–O bonds of p -methoxytoluene and p -methoxybenzyl alcohol in solution

M. Fujiwara and K. Toyomi

Citation: *The Journal of Chemical Physics* **107**, 9354 (1997); doi: 10.1063/1.475232

View online: <http://dx.doi.org/10.1063/1.475232>

View Table of Contents: <http://scitation.aip.org/content/aip/journal/jcp/107/22?ver=pdfcov>

Published by the [AIP Publishing](#)

---

### Articles you may be interested in

Gas-phase photodissociation of CH<sub>3</sub>COCN at 308 nm by time-resolved Fourier-transform infrared emission spectroscopy

J. Chem. Phys. **136**, 044302 (2012); 10.1063/1.3674166

Vibrationally mediated photodissociation of ethene isotopic variants preexcited to the fourth C–H stretch overtone

J. Chem. Phys. **125**, 133301 (2006); 10.1063/1.2217743

Photodissociation of the vinoxy radical through conical, and avoided, intersections

J. Chem. Phys. **117**, 7198 (2002); 10.1063/1.1507587

A mechanism of photodissociation of diphenylmethane to a diphenylmethyl radical in solution

J. Chem. Phys. **109**, 1359 (1998); 10.1063/1.476688

Picosecond real time study of the bimolecular reaction O ( <sup>3</sup> P ) + C<sub>2</sub>H<sub>4</sub> and the unimolecular photodissociation of CH<sub>3</sub>CHO and H<sub>2</sub>CO

J. Chem. Phys. **109**, 1293 (1998); 10.1063/1.476679

---



# Photodissociation of C–H and C–O bonds of *p*-methoxytoluene and *p*-methoxybenzyl alcohol in solution

M. Fujiwara and K. Toyomi

Department of Chemistry, Faculty of Science, Hiroshima University, Kagamiyama, Higashi-Hiroshima 739, Japan

(Received 7 July 1997; accepted 8 September 1997)

The photodissociation of *p*-methoxytoluene and *p*-methoxybenzyl alcohol at 266 nm in *n*-heptane solution is studied by nanosecond fluorescence and absorption spectroscopy. The formation of a *p*-methoxybenzyl radical is identified by its fluorescence which is induced by excitation at 308 nm. The yields of the radical are of the order of  $\sim 10^{-3}$  for dissociation of *p*-methoxytoluene and *p*-methoxybenzyl alcohol. The growth rate of  $1.5 \times 10^8 \text{ s}^{-1}$  for the radical is equal to the decay rate of  $(1.5 \pm 0.3) \times 10^8 \text{ s}^{-1}$  for the precursor fluorescence in dissociation of *p*-methoxytoluene, whereas the growth rate of  $> 1.0 \times 10^9 \text{ s}^{-1}$  for the radical is much faster than the decay rate of  $(1.8 \pm 0.3) \times 10^8 \text{ s}^{-1}$  for the precursor fluorescence in dissociation of *p*-methoxybenzyl alcohol. The formation of the radical depends linearly on the photolysis pulse fluence for dissociation of *p*-methoxytoluene and *p*-methoxybenzyl alcohol. The data show existence of two distinct dissociation channels. *p*-Methoxytoluene dissociates from thermally equilibrated levels of the  $S_1$  state after vibrational relaxation, whereas *p*-methoxybenzyl alcohol dissociates from vibrationally excited levels of the  $S_1$  state in competition with vibrational relaxation. The difference of these channels is explained on a model of electronic coupling between the precursor and product states in the geometry where the C–H and C–O bonds are stretched in a plane perpendicular to the benzene rings. For *p*-methoxytoluene, the  $S_1$  state does not correlate adiabatically to the ground state of the C–H bond fission products, so intersystem crossing or internal conversion precedes dissociation. For *p*-methoxybenzyl alcohol, avoided crossing between the  $\pi\pi^*$  (benzene) configuration and the  $np(O)\sigma^*(C-O)$  repulsive configuration results in the adiabatic potential-energy surface which evolves to the ground state of the C–O bond fission products allowing rapid dissociation. © 1997 American Institute of Physics. [S0021-9606(97)02646-9]

## I. INTRODUCTION

It is well known that photoemission in the electronically excited states of organic molecules occurs from their vibrational ground levels in the condensed phase. The rate constants of  $10^0$ – $10^9 \text{ s}^{-1}$  for emission are much smaller than those of  $\sim 10^{11} \text{ s}^{-1}$  for vibrational relaxation, and emission cannot compete with vibrational relaxation in vibrationally excited levels.

For photodissociation of organic molecules, toluene,<sup>1–4</sup> and benzyl alcohol<sup>5</sup> have been reported to yield a benzyl radical from highly vibrationally excited levels of the  $S_0$  states by excitation to the  $S_3$  states at 193 nm in the gas phase. The dissociation rates of  $(1.9 \pm 0.2) \times 10^6 \text{ s}^{-1}$  for toluene<sup>4</sup> and  $(1.7 \pm 0.2) \times 10^6 \text{ s}^{-1}$  for benzyl alcohol<sup>5</sup> have been measured along with the benzyl yield of 0.75 for toluene.<sup>4</sup> From these values, the rate constants of  $\sim 10^6 \text{ s}^{-1}$  for dissociation are deduced.

How about photodissociation in the condensed phase? If the rate constants for dissociation are of the order of  $\sim 10^6 \text{ s}^{-1}$  in vibrationally excited levels of the  $S_1$  states, dissociation may occur from the vibrational ground levels, not from vibrationally excited levels, of the  $S_1$  states by ultraviolet excitation. Whether this is the case or not is a problem that needs experimental investigation.

The present paper deals with the photodissociation of *p*-methoxytoluene and *p*-methoxybenzyl alcohol in *n*-heptane solution at room temperature. The nanosecond

fluorescence and absorption experiments are performed. Excitation of these molecules at 266 nm produces a *p*-methoxybenzyl radical. Its fluorescence is observed by excitation at 308 nm. The quantum yield and rate for the dissociation are measured. The number of photons necessary for the dissociation is determined. Two dissociation channels are identified. *p*-Methoxytoluene dissociates from thermally equilibrated levels of the  $S_1$  state after vibrational relaxation, whereas *p*-methoxybenzyl alcohol dissociates from vibrationally excited levels of the  $S_1$  state in competition with vibrational relaxation. The difference of the mechanisms is explained in terms of electronic coupling between the precursor and product states.

## II. EXPERIMENT AND SIMULATION CALCULATION

*p*-Methoxytoluene (Tokyo Chemical, >99%), *p*-methoxybenzyl alcohol (Kanto Chemical, >98%), and *p*-methoxybenzyl chloride (Tokyo Chemical) were distilled. Naphthalene (Nacalai Tesque) was recrystallized from ethanol. *n*-Heptane (Dojindo, spectroscopic) was used as received. The sample solutions, containing *p*-methoxytoluene ( $2.0 \times 10^{-3} \text{ mol dm}^{-3}$ ), *p*-methoxybenzyl alcohol ( $2.5 \times 10^{-3} \text{ mol dm}^{-3}$ ), and *p*-methoxybenzyl chloride ( $\sim 10^{-3} \text{ mol dm}^{-3}$ ) with *n*-heptane, were degassed by freeze–pump–thaw cycles. The molar extinction coefficients were measured with an absorption spectrophotometer (Hitachi U-3210).

For the two-pulse fluorescence measurement, a pulse of the fourth harmonic (266 nm, <0.5 ns rms jitter) of a Nd:YAG laser (Quanta-Ray GCR-11) was used as the photolysis light. The fluorescence was induced by a second pulse (308 nm) from a XeCl excimer laser (Lumonics 500). The laser power was attenuated with ND filters (Sigma FNDU-50C02-10, -20, -50) and measured with a thermopile monitor (Ophir 03A-P, DGX). The delay time was adjusted with a digital delay generator (EG&G PAR 9650, <0.1 ns rms jitter). The laser beams were focused on a 10×10 mm quartz cell coaxially. The fluorescence was collected into a monochromator (Ritsu MC-10N) and detected with a photomultiplier (Hamamatsu R636, 2.0 ns rise). A part of the 308 nm beam was directed on a PIN photodiode (Hamamatsu S1722-02, 5.8 ns rise). The output signals from both the photomultiplier and photodiode were simultaneously fed to separate channels of a digital oscilloscope (Tektronix 2440, 500 MHz sampling, <0.1 ns rms jitter), which was interfaced to a personal computer (NEC PC-9801UV) for data storage.

For the transient absorption measurement, the photolysis light was the 266 nm laser pulse. The white light was provided by a Xe arc lamp (Ushio UXL-500D-O). The laser and lamp beams were collimated on the cell at right angles with each other. The detection apparatus for the white light was the same as for the fluorescence. All experiments were run at room temperature (293 K).

The time profile of the radical fluorescence can be reproduced using convolution by the following expression:

$$S(t) = [F_{\text{grow}}(t) * I_{\text{pump}}(t)] \times I_{\text{probe}}(t) * F_{\text{decay}}(t) * R_{\text{detect}}(t). \quad (1)$$

The symbol \* means convolution.  $I_{\text{pump}}(t)$  and  $I_{\text{probe}}(t)$  are the intensity time profiles of the two excitation pulses. Their

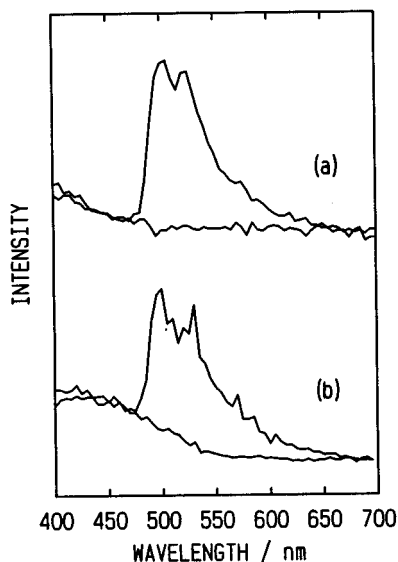


FIG. 1. Two-pulse fluorescence spectra of a *p*-methoxybenzyl radical observed by excitation with a 308 nm pulse at 1  $\mu$ s after excitation of (a) *p*-methoxytoluene and (b) *p*-methoxybenzyl alcohol with a 266 nm pulse. Upper curves are generated with both 266 and 308 nm pulses, while lower ones with only a 308 nm pulse.

best forms are Gaussian functions with widths (FWHM) of 4.5 and 4.0 ns, respectively.  $R_{\text{detect}}(t)$  is the response function of the detection system including the photomultiplier and digital oscilloscope. It is assumed to have a Gaussian form with a width of 3.5 ns.  $F_{\text{grow}}(t)$  is the population function of the ground-state radical, and  $F_{\text{decay}}(t)$  is the depopulation function of the excited-state radical, which is proportional to the decay of the radical fluorescence.

$$F_{\text{grow}}(t) = 1 - \exp(-k_{\text{grow}}t), \quad (2)$$

$$F_{\text{decay}}(t) = \exp(-k_{\text{decay}}t), \quad (3)$$

$k_{\text{grow}}$  is the growth rate constant of the ground-state radical that is to be determined, and  $k_{\text{decay}}$  is the decay rate constant of the excited-state radical which is fixed to be  $7.2 \times 10^6 \text{ s}^{-1}$ . The calculation is made with 0.2 ns increment.

### III. RESULTS

#### A. Identification of radical

In order to identify the fragment radical formed from photodissociation of *p*-methoxytoluene and *p*-methoxybenzyl alcohol, the two-pulse fluorescence and transient absorption spectra are measured.

The two-pulse fluorescence spectra, shown in Fig. 1, are observed by excitation with the 308 nm pulse after photolysis of *p*-methoxytoluene and *p*-methoxybenzyl alcohol with the 266 nm pulse. Excitation with the 308 nm pulse alone does not induce the fluorescence. The spectra exhibit a broad band at 510 nm, which is assigned to the *p*-methoxybenzyl radical and is similar to the band reported previously.<sup>6</sup> The fluorescence lifetimes, determined from photolysis of *p*-methoxytoluene and *p*-methoxybenzyl alcohol, are of a value of  $141 \pm 12 \text{ ns}$  and agree with the previous lifetime.<sup>6</sup> The fluorescence band disappears at a 100  $\mu$ s delay from the 266 to the 308 nm pulse. The result shows that C–H bond fission in *p*-methoxytoluene and C–O bond scission in *p*-methoxybenzyl alcohol occur to form the *p*-methoxybenzyl radical.

The transient absorption spectra are recorded by excitation of *p*-methoxytoluene and *p*-methoxybenzyl alcohol with the 266 nm pulse. However, the band assignable to the *p*-methoxybenzyl radical is obscured by broad bands in the 300–470 nm region, which are assigned to the  $T_1$  states of *p*-methoxytoluene and *p*-methoxybenzyl alcohol by comparison with the band of the  $T_1$  state of benzene.<sup>7</sup> The lifetimes of the  $T_1$  states are determined to be  $3.0 \pm 0.6 \mu\text{s}$  for *p*-methoxytoluene and  $2.9 \pm 0.6 \mu\text{s}$  for *p*-methoxybenzyl alcohol.

The two-pulse fluorescence and transient absorption measurements are performed by photolysis of *p*-methoxybenzyl chloride with the 266 nm pulse. This molecule has been reported to yield the *p*-methoxybenzyl radical.<sup>6,8</sup> The same fluorescence band (with the same lifetime) as in Fig. 1 is observed by excitation with the 308 nm pulse. An absorption band is recorded at 288 nm, which is associated with the *p*-methoxybenzyl radical.<sup>6,8,9</sup> The fluorescence and absorption bands disappear at a 100  $\mu$ s delay.

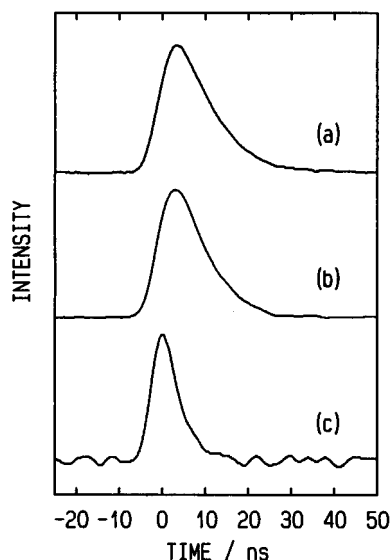


FIG. 2. Time evolution of fluorescence of (a) *p*-methoxytoluene and (b) *p*-methoxybenzyl alcohol recorded by excitation with a 266 nm pulse. (c) Time evolution of a 266 nm pulse. Monitoring wavelength: (a) and (b) 300 nm.

From the observation it is confirmed that the *p*-methoxybenzyl radical is formed from dissociation of *p*-methoxytoluene and *p*-methoxybenzyl alcohol.

### B. Radical yields

The quantum yields of the *p*-methoxybenzyl radical from dissociation of *p*-methoxytoluene, *p*-methoxybenzyl alcohol, and *p*-methoxybenzyl chloride are estimated as follows: Firstly, the ratio of the *p*-methoxybenzyl yields from dissociation of *p*-methoxytoluene, *p*-methoxybenzyl alcohol, and *p*-methoxybenzyl chloride is measured by comparing its fluorescence intensities by excitation with the 308 nm pulse after photolysis with the 266 nm pulse. Secondly, the *p*-methoxybenzyl yield from dissociation of *p*-methoxybenzyl chloride is measured by comparison with the naphthalene triplet one as the standard from its absorbance by excitation with the 266 nm pulse. The extinction coefficients used are  $1.1 \times 10^4 \text{ dm}^3 \text{ mol}^{-1} \text{ cm}^{-1}$  (288 nm)<sup>9</sup> for the *p*-methoxybenzyl radical and  $1.4 \times 10^4 \text{ dm}^3 \text{ mol}^{-1} \text{ cm}^{-1}$  (415 nm)<sup>10</sup> for naphthalene triplet. The intersystem crossing yield for naphthalene is 0.68.<sup>10</sup> In this way, an estimate for the *p*-methoxybenzyl yields of  $\sim 1.3 \times 10^{-3}$ ,  $\sim 2.9 \times 10^{-3}$ , and 0.38 is made from dissociation of *p*-methoxytoluene, *p*-methoxybenzyl alcohol, and *p*-methoxybenzyl chloride, respectively.

### C. Rates of $S_1$ decay and radical growth

To obtain knowledge of excited states that lead to dissociation, the growth rates of the *p*-methoxybenzyl radical are measured along with the decay rates of the  $S_1$  states of *p*-methoxytoluene and *p*-methoxybenzyl alcohol.

For *p*-methoxytoluene and *p*-methoxybenzyl alcohol, the decay rates of thermally equilibrated levels of the  $S_1$

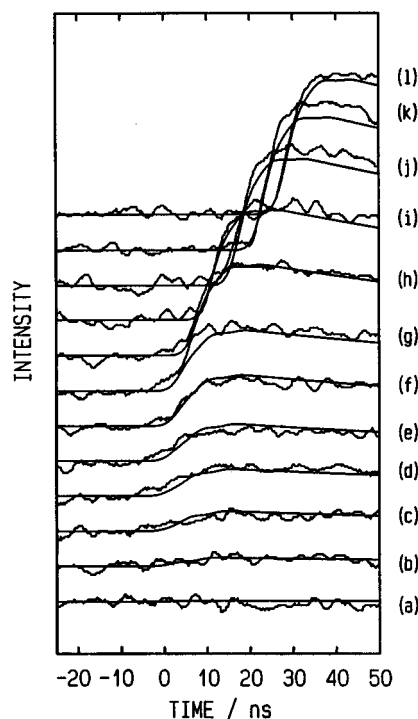


FIG. 3. Observed and calculated fluorescence time profiles of a *p*-methoxybenzyl radical at various delay times from a 266 to a 308 nm pulse. Fluorescence is induced by excitation with a 308 nm pulse after excitation of *p*-methoxytoluene at 0 ns with a 266 nm pulse. Monitoring wavelength is set at 510 nm. Delay times of a 308 nm pulse: (a) -11.8; (b) -4.8; (c) -1.8; (d) -0.6; (e) 0.8; (f) 2.6; (g) 3.4; (h) 7.4; (i) 11.2; (j) 17.8; (k) 23.4; (l) 28.6 ns.

states can be determined as those of the fluorescence from the  $S_1$  states. The fluorescence time profiles of *p*-methoxytoluene and *p*-methoxybenzyl alcohol, observed by excitation with the 266 nm pulse, are shown in Fig. 2. Thermally equilibrated levels of the  $S_1$  states are found to decay with rates of  $(1.5 \pm 0.3) \times 10^8 \text{ s}^{-1}$  for *p*-methoxytoluene and  $(1.8 \pm 0.3) \times 10^8 \text{ s}^{-1}$  for *p*-methoxybenzyl alcohol.

For the (ground-state) *p*-methoxybenzyl radical, its growth rates are evaluated from the dependence of its fluorescence time profile on the delay from the 266 nm (photolysis) to the 308 nm (probe) pulse. The jitter of the 266 nm pulse is limited to be  $< 0.5 \text{ ns}$ , while the delay of the 308 nm pulse is calibrated by the photodiode signal. Unknown fluorescence, observed by alternative excitation with either the 266 or 308 nm pulse, is subtracted from fluorescence, obtained by simultaneous excitation with both the 266 and 308 nm pulses, after calibration of the delay.

The fluorescence time profiles of the *p*-methoxybenzyl radical at various delays of the 308 nm pulse are shown in Fig. 3 for dissociation of *p*-methoxytoluene. It is noted that the intensity and delay of the fluorescence change with the delay of the 308 nm pulse. The fluorescence intensity begins to grow at a -1.8 ns delay of the 308 nm pulse [Fig. 3(c)], and reaches a plateau at a 17.8 ns delay of this pulse [Fig. 3(j)]. The intensity growth is accompanied with the delay of

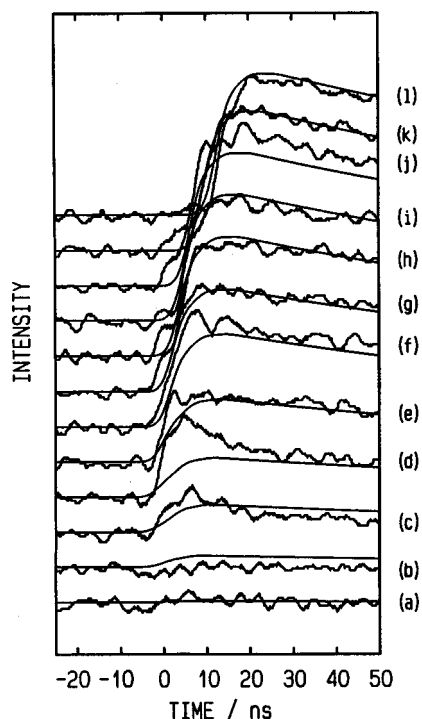


FIG. 4. Observed and calculated fluorescence time profiles of a *p*-methoxybenzyl radical at various delay times from a 266 to a 308 nm pulse. Fluorescence is induced by excitation with a 308 nm pulse after excitation of *p*-methoxybenzyl alcohol at 0 ns with a 266 nm pulse. Monitoring wavelength is set at 510 nm. Delay times of a 308 nm pulse: (a) -13.2; (b) -6.8; (c) -3.8; (d) -2.6; (e) -0.8; (f) 1.2; (g) 2.1; (h) 3.9; (i) 4.9; (j) 6.5; (k) 9.5; (l) 12.7 ns.

the fluorescence itself. After a 17.8 ns delay of the 308 nm pulse, the fluorescence intensity does not change but the fluorescence delays following the 308 nm pulse. To simulate the fluorescence time profiles in Fig. 3, the growth rate of  $1.5 \times 10^8 \text{ s}^{-1}$  for the *p*-methoxybenzyl radical can be satisfactorily used, which is equal to the decay rate for the fluorescence of *p*-methoxytoluene. This shows that the dissociation channel of the C-H bond occurs from thermally equilibrated levels of the  $S_1$  state for *p*-methoxytoluene.

The fluorescence time profiles of the *p*-methoxybenzyl radical at various delays of the 308 nm pulse are shown in Fig. 4 for dissociation of *p*-methoxybenzyl alcohol. The fluorescence intensity begins to grow at a -6.8 ns delay of the 308 nm pulse [Fig. 4(b)], and the intensity growth is completed at a 4.9 ns delay of this pulse [Fig. 4(i)]. The fluorescence does not delay during its intensity growth. After a 4.9 ns delay of the 308 nm pulse, the fluorescence delays following the 308 nm pulse without change of its intensity. Simulation with the growth rate of  $1.8 \times 10^8 \text{ s}^{-1}$  for the *p*-methoxybenzyl radical, the value equal to the decay rate for the fluorescence of *p*-methoxybenzyl alcohol, does not reproduce the experimental results. Instead, the growth rate of  $> 1.0 \times 10^9 \text{ s}^{-1}$  is found to be necessary to simulate the fluorescence time profiles in Fig. 4. It is clear that the growth rate for the *p*-methoxybenzyl radical is much faster than the decay rate for the fluorescence of *p*-methoxybenzyl alcohol.

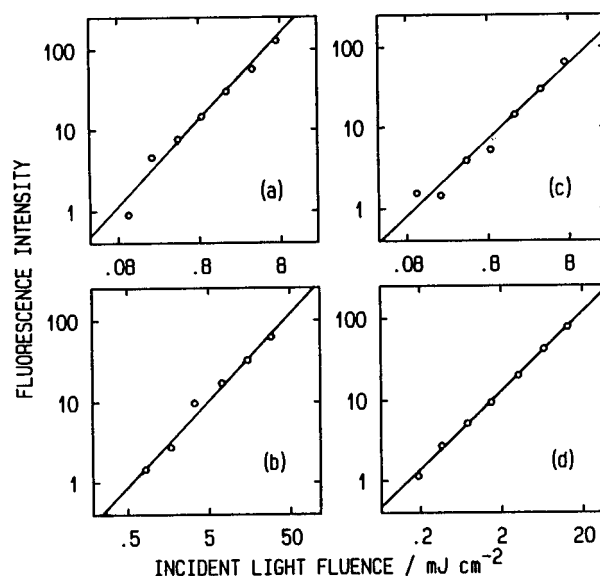


FIG. 5. Logarithmic plots of a fluorescence intensity of a *p*-methoxybenzyl radical versus (a) and (c) 266 and (b) and (d) 308 nm pulse fluences. Fluorescence is induced by excitation with a 308 nm pulse at 1  $\mu\text{s}$  after excitation of (a) and (b) *p*-methoxytoluene and (c) and (d) *p*-methoxybenzyl alcohol with a 266 nm pulse. Monitoring wavelength: 510 nm.

This leads to the explanation that the dissociation channel of the C-O bond occurs from vibrationally excited levels of the  $S_1$  state for *p*-methoxybenzyl alcohol.

The analysis of the fluorescence time profiles assumes that one dissociation channel with one growth rate of the *p*-methoxybenzyl radical exists for each dissociation process of *p*-methoxytoluene and *p*-methoxybenzyl alcohol. Nonetheless, the observed and calculated time profiles agree to a great extent, when the fluctuations of the 266 and 308 nm pulse fluences are taken into account. This means that the major dissociation channel is identified, but this does not preclude a possibility that minor dissociation channels exist.

#### D. One- or two-photon photochemistry

The number of photons required for excitation of *p*-methoxytoluene and *p*-methoxybenzyl alcohol to their dissociative states is determined from the dependence of the fluorescence intensity of the *p*-methoxybenzyl radical on the fluences of the 266 nm (photolysis) and 308 nm (probe) pulses.

The logarithmic plots of the fluorescence intensity of the *p*-methoxybenzyl radical versus the 266 nm pulse fluence are shown in Figs. 5(a) and 5(c) for dissociation of *p*-methoxytoluene and *p*-methoxybenzyl alcohol. Observed points are linearly fitted with slopes of  $1.08 \pm 0.24$  for dissociation of *p*-methoxytoluene and  $0.94 \pm 0.23$  for dissociation of *p*-methoxybenzyl alcohol. It is evident that the dissociation occurs by 266 nm one-photon excitation.

The *p*-methoxybenzyl fluorescence intensity is plotted as a function of the 308 nm pulse fluence in Figs. 5(b) and 5(d) for dissociation of *p*-methoxytoluene and *p*-methoxybenzyl alcohol. Linear fitting results in slopes of  $1.06 \pm 0.21$  for dis-

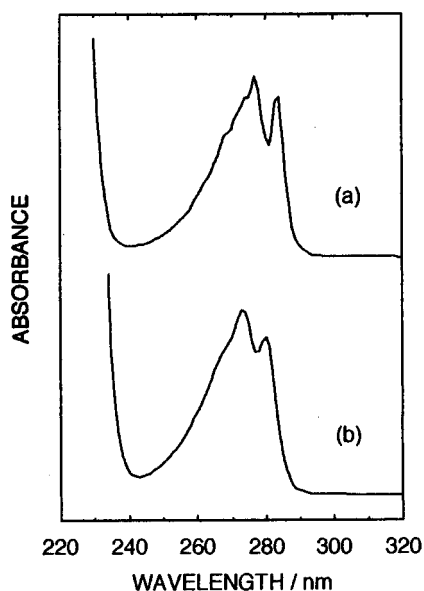


FIG. 6. Absorption spectra of (a) *p*-methoxytoluene and (b) *p*-methoxybenzyl alcohol.

sociation of *p*-methoxytoluene and  $0.97 \pm 0.06$  for dissociation of *p*-methoxybenzyl alcohol. It is shown that one 308 nm photon is required to populate the fluorescent state of the radical. A possibility is excluded that two-photon absorption occurs in the duration of the 308 nm pulse for formation of the radical and population of its fluorescent state.

#### IV. DISCUSSION

##### A. Excitation wavelength and bond dissociation energies

In Fig. 6 are shown the absorption spectra of *p*-methoxytoluene and *p*-methoxybenzyl alcohol. Weak bands appear with maxima at  $36\,000\text{ cm}^{-1}$  ( $2.0 \times 10^3\text{ dm}^3\text{ mol}^{-1}\text{ cm}^{-1}$ ) for *p*-methoxytoluene and  $36\,500\text{ cm}^{-1}$  ( $1.2 \times 10^3\text{ dm}^3\text{ mol}^{-1}\text{ cm}^{-1}$ ) for *p*-methoxybenzyl alcohol, and correspond to the transitions to the  $S_1(^1B_{2u})$  state in benzene which are allowed due to vibronic coupling with the  $520\text{ cm}^{-1}e_{2g}$  vibration in the  $D_{6h}$  symmetry.<sup>11</sup> The  $0 \rightarrow 0$  transitions are seen at  $35\,200\text{ cm}^{-1}$  for *p*-methoxytoluene and  $35\,700\text{ cm}^{-1}$  for *p*-methoxybenzyl alcohol. The  $0 \rightarrow n$  transitions ( $n = 1, 2, 3$ ) in the  $920\text{ cm}^{-1}a_{1g}$  vibration are also seen for *p*-methoxytoluene and *p*-methoxybenzyl alcohol. By absorption of one 266 nm photon ( $37\,600\text{ cm}^{-1}$ ), *p*-methoxytoluene and *p*-methoxybenzyl alcohol are excited to the vibrational levels of  $S_1$  states that are above the vibrational ground levels by 2400 and  $1900\text{ cm}^{-1}$ , respectively.

The dissociation of the C–H bond of *p*-methoxytoluene and the C–O bond of *p*-methoxybenzyl alcohol is shown to occur by one-photon excitation at 266 nm [Figs. 5(a) and 5(c)]. The bond dissociation energies are estimated to be  $30\,800\text{ cm}^{-1}$  for  $\text{CH}_3\text{OC}_6\text{H}_4\text{CH}_2\text{--H}$  and  $28\,500\text{ cm}^{-1}$  for  $\text{CH}_3\text{OC}_6\text{H}_4\text{CH}_2\text{--OH}$  from those for  $\text{C}_6\text{H}_5\text{CH}_2\text{--H}$  ( $30\,800\text{ cm}^{-1}$ ),  $\text{CH}_3\text{CH}_2\text{--H}$  ( $35\,000\text{ cm}^{-1}$ ), and  $\text{CH}_3\text{CH}_2\text{--OH}$  ( $32\,700\text{ cm}^{-1}$ ).<sup>12</sup> Excitation with one 266 nm photon

( $37\,600\text{ cm}^{-1}$ ) populates the  $S_1$  states of *p*-methoxytoluene ( $\nu_0 = 35\,200\text{ cm}^{-1}$ ) and *p*-methoxybenzyl alcohol ( $\nu_0 = 35\,700\text{ cm}^{-1}$ ) with excess vibrational energies. Clearly, the energies that the molecules possess are sufficient to fragment them into the radical.

##### B. Adiabatic potential-energy surfaces

For *p*-methoxytoluene, a channel leading to dissociation is shown to occur with the yield of  $\sim 1.3 \times 10^{-3}$  from thermally equilibrated levels of the  $S_1$  state (Fig. 3). Vibrational relaxation is a dominant energy dissipation mechanism from the Franck–Condon state, and dissociation is allowed to occur after vibrational relaxation. For *p*-methoxybenzyl alcohol, a channel leading to dissociation is found to occur with the yield of  $\sim 2.9 \times 10^{-3}$  from vibrationally excited levels of the  $S_1$  state (Fig. 4). An energy relaxation mechanism from vibrationally excited levels of the  $S_1$  state consists of two channels: One that crosses to a potential-energy surface leading to dissociation, and a second that relaxes vibrationally to thermally equilibrated levels of the  $S_1$  state.

The difference of the dissociation processes between *p*-methoxytoluene and *p*-methoxybenzyl alcohol may be understood by considering the symmetry of the potential-energy surfaces along fission of the C–H and C–O bonds.<sup>13–17</sup> The most favorable geometry of stretch of the C–H and C–O bonds that leads to the planar structure of the benzyl radical is a one in which it occurs in a plane perpendicular to the benzene rings of toluene and benzyl alcohol (see Figs. 7 and 8). Since the energy of this geometry is comparable to the energies of other distorted geometries in which the C–H and C–O bonds are stretched, the assumption is made that the reaction coordinates of fission of the C–H and C–O bonds lie in the symmetry plane perpendicular to the benzene rings of *p*-methoxytoluene and *p*-methoxybenzyl alcohol.

For *p*-methoxytoluene, photoexcitation promotes the molecule to the  $S_1[^1B_{2u}, \pi\pi^*(\text{benzene})]$  state which is of  $A''$  symmetry relative to the symmetry plane perpendicular to the benzene ring. The ground ( $^2B_2$ ) and excited ( $^2A_2$ ) states of the *p*-methoxybenzyl radical possess  $A'$  and  $A''$  symmetries, respectively. In the conventional classification of the  $C_{2v}$  point group to which the benzyl radical belongs,<sup>18,19</sup> the plane of the benzene ring of the *p*-methoxybenzyl radical is represented as the  $xz$  plane and that plane perpendicular to the benzene ring which is the symmetry plane for the present model is represented as the  $yz$  plane with the primary symmetry axis being the  $z$  axis. The  $^2B_2$  and  $^2A_2$  state labels are the symmetry representations for the  $C_{2v}$  point group, while the  $A'$  and  $A''$  labels are the symmetry representations with respect to the symmetry plane perpendicular to the benzene ring. The symmetry of the ground-state ( $^2S$ ) H atom is  $A'$ . Thus, the  $S_1(A'')$  potential-energy surface of the precursor does not correlate adiabatically to the ground ( $^2B_2 + ^2S, A'$ ) state of the products, but does correlate to the excited ( $^2A_2 + ^2S, A''$ ) state of the products. If the  $S_1$  state were to participate in C–H bond fission, a symmetry-imposed energy barrier must be overcome. As a result, C–H bond fis-

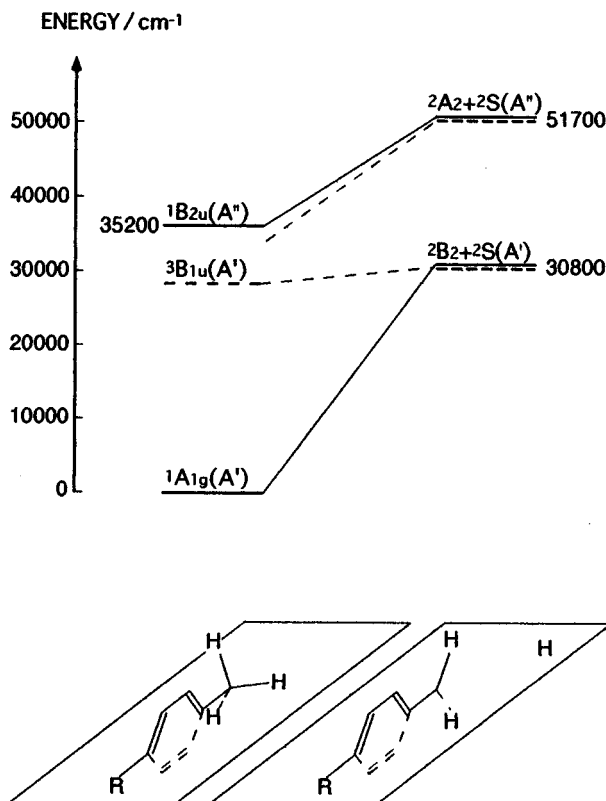


FIG. 7. A state correlation diagram for C-H bond fission of *p*-methoxytoluene. States of *p*-methoxytoluene and a *p*-methoxybenzyl radical are represented with corresponding ones of benzene ( $D_{6h}$ ) and a benzyl radical ( $C_{2v}$ ), respectively. Symmetry representations relative to a symmetry plane are noted for singlet (solid lines) and triplet (broken lines) states in parentheses. A benzene ring is perpendicular to a symmetry plane, on which a C-H bond lies.  $R = \text{OCH}_3$ .

sion cannot occur adiabatically from the  $S_1$  surface. It is allowed to proceed via intersystem crossing to vibrationally excited levels of the  $T_1(^3B_{1u})$  state (of  $A'$  symmetry). Alternatively, it may proceed via internal conversion to vibrationally excited levels of the  $S_0$  state (of  $A'$  symmetry). Intersystem crossing or internal conversion cannot compete effectively with vibrational relaxation in the  $S_1$  surface, so C-H bond cleavage follows vibrational relaxation. This accounts for the experimental observable that the dissociation rate is determined by the decay rate of thermally equilibrated levels of the  $S_1$  state. In addition, since dissociation occurs actually from vibrationally excited levels of the  $T_1$  or  $S_0$  state, the low dissociation yield of  $\sim 1.3 \times 10^{-3}$  results from competition with vibrational relaxation of which the rate is expected to be  $\sim 10^{11} \text{ s}^{-1}$  in the  $T_1$  or  $S_0$  state.

In contrast, for dissociation of *p*-methoxybenzyl alcohol, the  $S_1[{}^1B_{2u}, \pi\pi^*(\text{benzene})]$  state of the precursor possesses  $A''$  symmetry relative to the symmetry plane perpendicular to the benzene ring. The dissociative [ $np(\text{O})\sigma^*(\text{C-O})$ ] state of alkyl alcohol ( $\nu_0 \sim 55\,000 \text{ cm}^{-1}$ ) is of  $A''$  symmetry with respect to this symmetry plane when the O-H bond lies in this symmetry plane. The symmetry of the ground-state ( ${}^2\Pi$ ) OH radical is  $A' + A''$ . Thus, avoided crossing occurs be-

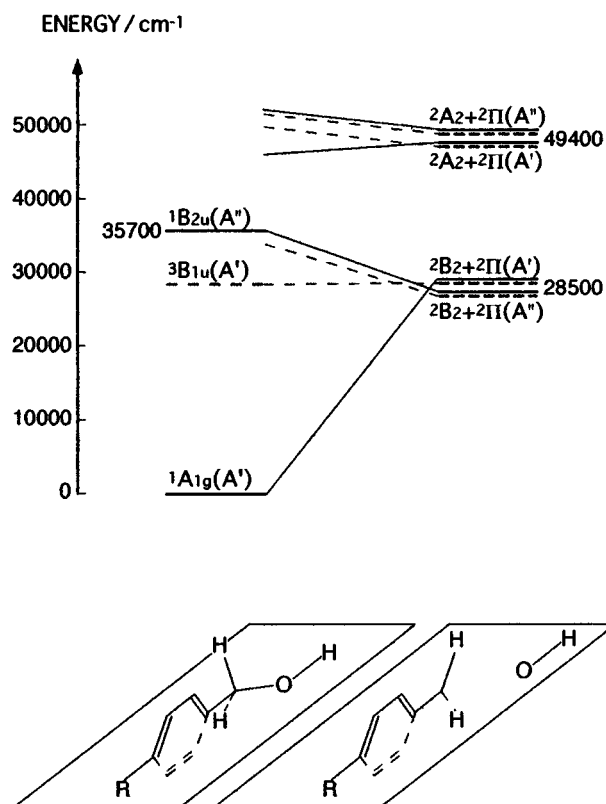


FIG. 8. A state correlation diagram for C-O bond fission of *p*-methoxybenzyl alcohol. States of *p*-methoxybenzyl alcohol and a *p*-methoxybenzyl radical are represented with corresponding ones of benzene ( $D_{6h}$ ) and a benzyl radical ( $C_{2v}$ ), respectively. Symmetry representations relative to a symmetry plane are noted for singlet (solid lines) and triplet (broken lines) states in parentheses. A benzene ring is perpendicular to a symmetry plane, on which C-O and O-H bonds lie.  $R = \text{OCH}_3$ .

tween the  $\pi\pi^*(\text{benzene})(A'')$  electronic configuration and the  $np(\text{O})\sigma^*(\text{C-O})(A'')$  repulsive electronic configuration at the geometry of the stretched C-O bond. It results in the  $A''$  potential-energy surface which evolves adiabatically from  $\pi\pi^*(\text{benzene})$  character in the Franck-Condon region to  $np(\text{O})\sigma^*(\text{C-O})$  character beyond the barrier along the reaction coordinate of C-O bond fission. Rapid C-O bond fission can proceed directly on the resulting  $A''$  adiabatic potential-energy surface from the  $S_1({}^1B_{2u})$  state of the precursor to the ground ( ${}^2B_2 + {}^2\Pi$ ) state of the products. In this way, the presence of an out-of-plane *p* orbital on the O atom allows an adiabatic reaction pathway consistent with rapid C-O bond fission. In addition, since there exists an exit channel barrier on the  $A''$  surface, statistical partitioning of excess vibrational energy is required for crossing over the barrier to C-O bond fission. This predicts that dissociation proceeds from vibrationally excited levels of the  $S_1$  state after intramolecular vibrational redistribution. The low dissociation yield of  $\sim 2.9 \times 10^{-3}$  is accounted for by competition with vibrational relaxation whose rate is expected to be  $\sim 10^{11} \text{ s}^{-1}$  in the  $S_1$  state.

The present model requires that the H atom of *p*-methoxytoluene and the O-H bond of *p*-methoxybenzyl

alcohol lie in the symmetry plane perpendicular to the benzene rings (Figs. 7 and 8). The energy barriers to torsion of the methyl group for the *p*-fluorotoluene are  $4.8\text{ cm}^{-1}$  in the  $S_0$  state and  $33.7\text{ cm}^{-1}$  in the  $S_1$  state.<sup>20</sup> The energy difference from the trans to the gauche conformation with respect to the C–O bond for ethyl alcohol is  $41.2 \pm 5.0\text{ cm}^{-1}$  in the  $S_0$  state.<sup>21</sup> Therefore, the H atom of *p*-methoxytoluene and the O–H bond of *p*-methoxybenzyl alcohol will be restricted in the symmetry plane perpendicular to the benzene rings with high probabilities, though the explanation does not consider hyperconjugation involving the benzene rings.

### C. Other dissociation mechanisms

The photodissociation pathway of *p*-methoxytoluene in the liquid phase may be similar to that of toluene,<sup>1–4</sup> benzyl alcohol,<sup>5</sup> and benzyl halides<sup>22</sup> in the gas phase. In the liquid phase, the fission of the C–H bond occurs ultimately from vibrationally excited levels of the  $T_1$  or  $S_0$  state after intersystem crossing or internal conversion. The actual dissociation rate from vibrationally excited levels of the  $T_1$  or  $S_0$  state is not measured. It is limited by the decay rate of thermally equilibrated levels of the  $S_1$  state. The dissociation is a minor channel ( $\sim 10^{-3}$  yield), since the rapid vibrational relaxation process ( $\sim 10^{11}\text{ s}^{-1}$ ) exists. In the gas phase, the fission of the C–H, C–O, and C–X bonds ( $X=\text{Cl}, \text{Br}, \text{I}$ ) occurs from highly vibrationally excited levels of the  $S_0$  states by internal conversion after excitation to the  $S_3$  states at 193 nm. The measured dissociation rates ( $\sim 10^6\text{ s}^{-1}$ ) are predicted by the statistical unimolecular dissociation theory on the assumption that the electronic energies in the photoexcited states are distributed over the vibrational modes. The dissociation is a dominant energy dissipation process (0.75 yield) from the excited state for toluene.

The photodissociation mechanism of *p*-methoxybenzyl alcohol in the liquid phase seems to be different from that of 1- and 2-(halomethyl)naphthalenes in the liquid phase.<sup>23,24</sup> For *p*-methoxybenzyl alcohol, the fission of the C–O bond is characterized by adiabatic crossing to the  $np(\text{O})\sigma^*(\text{C–O})$  potential-energy surface. This is because the lowest excited state of alkyl alcohol is the  $np(\text{O})\sigma^*(\text{C–O})$  one, and because the  $np(\text{O})\rightarrow\sigma^*(\text{C–O})$  transition is of energy of  $\sim 55\,000\text{ cm}^{-1}$ . For 1- and 2-(halomethyl)naphthalenes, the fission of the C–X bonds ( $X=\text{Cl}, \text{Br}$ ), occurring after excitation to the  $S_2$  states at 266 or 299 nm, is distinguished by intersystem crossing to upper triplet states which are themselves or cross to dissociative  $\sigma\sigma^*$  triplet states.

### V. CONCLUSIONS

Excitation of *p*-methoxytoluene and *p*-methoxybenzyl alcohol at 266 nm produces a *p*-methoxybenzyl radical in *n*-heptane solution. The growth rate of the radical is equal to the decay rate of the precursor fluorescence for dissociation of *p*-methoxytoluene, whereas the former is much faster than

the latter for dissociation of *p*-methoxybenzyl alcohol. The formation of the radical depends linearly on the photolysis pulse fluence for the dissociation of *p*-methoxytoluene and *p*-methoxybenzyl alcohol. The observation shows existence of two dissociation channels. *p*-Methoxytoluene dissociates from thermally equilibrated levels of the  $S_1$  state after vibrational relaxation, whereas *p*-methoxybenzyl alcohol dissociates from vibrationally excited levels of the  $S_1$  state in competition with vibrational relaxation. The difference of these channels is explained on a model of electronic coupling between the precursor and product states. For *p*-methoxytoluene, the  $S_1$  state does not correlate adiabatically to the ground state of the C–H bond fission products, so intersystem crossing or internal conversion precedes dissociation. For *p*-methoxybenzyl alcohol, the adiabatic potential energy surface, evolving from the  $S_1$  state to the ground state of the C–O bond fission products, allows rapid dissociation along it.

<sup>1</sup>N. Ikeda, N. Nakashima, and K. Yoshihara, *J. Chem. Phys.* **82**, 5285 (1985).

<sup>2</sup>K. Tsukiyama and R. Bersohn, *J. Chem. Phys.* **86**, 745 (1987).

<sup>3</sup>Y. Kajii, K. Obi, I. Tanaka, N. Ikeda, N. Nakashima, and K. Yoshihara, *J. Chem. Phys.* **86**, 6115 (1987).

<sup>4</sup>U. Brand, H. Hippler, L. Lindemann, and J. Troe, *J. Phys. Chem.* **94**, 6305 (1990).

<sup>5</sup>P. K. Chowdhury, *J. Phys. Chem.* **98**, 13112 (1994).

<sup>6</sup>K. Tokumura, T. Ozaki, M. Udagawa, and M. Itoh, *J. Phys. Chem.* **93**, 161 (1989).

<sup>7</sup>N. Nakashima, M. Sumitani, I. Ohmine, and K. Yoshihara, *J. Chem. Phys.* **72**, 2226 (1980).

<sup>8</sup>K. Tokumura, T. Ozaki, H. Nosaka, Y. Saigusa, and M. Itoh, *J. Am. Chem. Soc.* **113**, 4974 (1991).

<sup>9</sup>R. F. C. Claridge and H. Fischer, *J. Phys. Chem.* **87**, 1960 (1983).

<sup>10</sup>I. Carmichael and G. L. Hug, in *CRC Handbook of Organic Photochemistry*, edited by J. C. Scaiano (CRC, Boca Raton, Florida, 1989), Vol. 1, Chap. 16.

<sup>11</sup>J. Petruska, *J. Chem. Phys.* **34**, 1120 (1961).

<sup>12</sup>D. Griller and J. M. Kanabus-Kaminska, in *CRC Handbook of Organic Photochemistry*, edited by J. C. Scaiano (CRC, Boca Raton, Florida, 1989), Vol. 2, Chap. 17.

<sup>13</sup>L. Salem, *J. Am. Chem. Soc.* **96**, 3486 (1974).

<sup>14</sup>N. J. Turro, W. E. Farneth, and A. Devaquet, *J. Am. Chem. Soc.* **98**, 7425 (1976).

<sup>15</sup>S. S. Hunnicutt, L. D. Waits, and J. A. Guest, *J. Phys. Chem.* **95**, 562 (1991).

<sup>16</sup>M. D. Person, P. W. Kash, S. A. Schofield, and L. J. Butler, *J. Chem. Phys.* **95**, 3843 (1991).

<sup>17</sup>M. D. Person, P. W. Kash, and L. J. Butler, *J. Chem. Phys.* **97**, 355 (1992).

<sup>18</sup>J. E. Rice, N. C. Handy, and P. J. Knowles, *J. Chem. Soc. Faraday Trans. II* **83**, 1643 (1987).

<sup>19</sup>F. Negri, G. Orlandi, F. Zerbetto, and M. Z. Zgierski, *J. Chem. Phys.* **93**, 600 (1990).

<sup>20</sup>K. Okuyama, N. Mikami, and M. Ito, *J. Phys. Chem.* **89**, 5617 (1985).

<sup>21</sup>P. K. Kakar and C. R. Quade, *J. Chem. Phys.* **72**, 4300 (1980).

<sup>22</sup>A. Freedman, S. C. Yang, M. Kawasaki, and R. Bersohn, *J. Chem. Phys.* **72**, 1028 (1980).

<sup>23</sup>D. F. Kelley, S. V. Milton, D. Huppert, and P. M. Rentzepis, *J. Phys. Chem.* **87**, 1842 (1983).

<sup>24</sup>E. F. Hilinski, D. Huppert, D. F. Kelley, S. V. Milton, and P. M. Rentzepis, *J. Am. Chem. Soc.* **106**, 1951 (1984).